IEEE/CSC & ESAS EUROPEAN SUPERCONDUCTIVITY NEWS FORUM (ESNF), No. 18, October 2011
Submitted to ESNF August 12, 2011; accepted September 29, 2011. Reference ST275, Category 4.
Published in *Journal of Low Temperature Physics* **167**, Numbers 3-4, 410-415, (2012)

Response of the Killed Electrode in STJ X-ray Detectors

V.A. Andrianov[1] and V.P. Gorkov[2]

[1] *Lomonosov Moscow State University, Skobeltsyn Institute of Nuclear Physics, 119991 Moscow, Russian Federation*
[2] *Lomonosov Moscow State University, Faculty of Computational Mathematics and Cybernetics, 119991 Moscow, Russian Federation*

The signals of STJ detectors Ti/Nb/Al,AlO_x/Al/Nb/NbN with killed Ti/Nb electrode were studied as a function of the bias voltage, the energy of the absorbed quanta and the thickness of the electrodes. The nonlinearity of the energy calibration for the killed electrode signal had a positive curvature due to the quasiparticles self-recombination losses and 2Δ-phonon exchange. Suppression of residual signals of the killed electrode was achieved by increasing the thickness of this electrode.
PACS numbers: 85.25.Am, 74.50.+r.

1. INTRODUCTION

X-ray detectors based on superconducting tunnel junctions (STJ detectors) have three main designs: detectors with identical electrodes, which work in multiple tunneling mode, strip STJ detectors, and detectors with killed electrode [1, 2]. Detectors with killed electrode consist of two electrodes with essential different properties. The detector signal arises from absorption of the quantum in the main electrode, which usually has a multilayer structure. The signals of the opposite killed electrode should be suppressed due to the presence of the quasiparticle trapping layer placed at the side opposite to the tunnel barrier. Two potential advantages of these detectors are the absence of line doubling caused by quantum absorption in the both electrodes and the short duration of the signals.

In previous studies, we proposed the STJ detector design with killed electrode on the basis of the additional titanium trapping layer [3]. The general sequence of layers is described by the formula Ti/Nb/Al,AlO_x/Al/Nb/NbN. The bottom killed electrode consistes of two layers: a Ti trapping layer and a thicker Nb layer. The main top electrode has three layers: thin Al trapping layer, the main absorbing Nb layer, and the outer NbN layer.

Unfortunately, the experiment has shown that the full suppression of the signals of the killed electrode does not occur and that this signal have the amplitudes of 5-10 % of the main signals amplitude depending on the sample. To clarify this situation, the signals of STJ detectors with killed Ti/Nb electrode were studied as a function of the bias voltage, the energy of the absorbed quanta, and the thickness of Nb-layers.

2. EXPERIMENT

The samples of STJ detectors Ti/Nb/Al,AlO_x/Al/Nb/NbN were fabricated by magnetron sputtering in Ar. The STJ detectors with the rhombic shape of the electrodes and areas S = 6400 and S = 20000 μm^2 were studied. The normal resistance of the tunnel barrier was $R_NS \approx 400$ Ω μm^2. The layer thicknesses were as follows: Ti and NbN (30 nm each), base Nb layer (100 or 150 nm), Al/AlO_x oxide layer (4 nm/2 nm), top Nb layer (150, 200, or 250 nm), and trapping top Al layer (11-13 nm). The superconducting gaps for the bottom and top electrodes were $\Delta_{base} = 1.36$ meV and $\Delta_{top} \approx 0.95$ meV. The best resolution was of about 90 eV at the 5.9 keV line. The details of the sample preparation and experimental setup are given elsewhere [3,4].

The detectors were tested at temperature of 1.25 K. The samples were irradiated by MnK_α and MnK_β X-rays (5.9 and 6.4 keV) of a ^{55}Fe radioactive source and by fluorescent TiK_α and TiK_β X-rays (4.5 and 4.9 keV) from a Ti

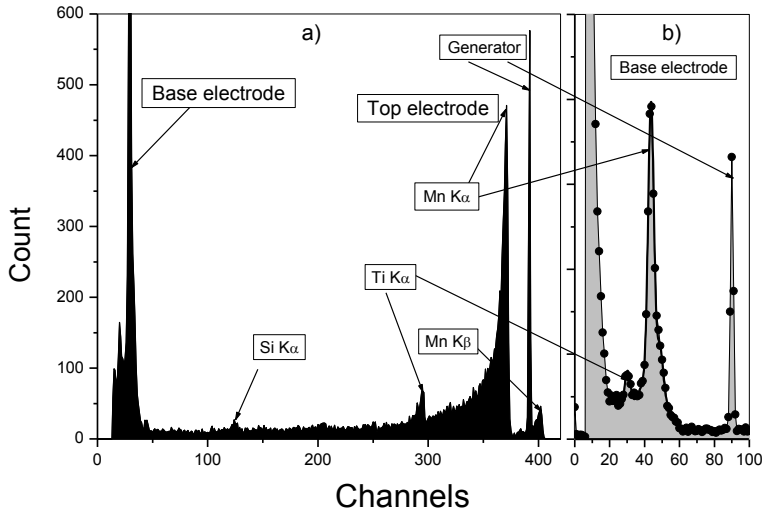

Fig. 1. Pulse height spectrum of the STJ detector Ti/Nb/Al,AlO_x/Al/Nb/NbN at $V_d = 0.59$ mV: (a) total spectrum and (b) subspectrum of the bottom electrode. Layer thicknesses are 30/150/4,2/13/250/30 nm; the detector area is 6400 μm^2.

foil shield placed around the source. The typical spectrum of the STJ detector of area S = 6400 μm^2 is shown in figure 1a. The Mn K_α, Mn K_β, and Ti K_α lines corresponding to X-ray absorption in the top electrode are clearly seen. The spectrum also contains the fluorescent Si K_α line caused by X-ray absorption in the silicon substrate. In the low amplitude region, the spectrum contains the peak corresponding to X-ray absorption in the bottom electrode. The amplitudes of these signals are smaller than those of the top electrode by a factor of ~13. Thus, the killed electrode signal is not completely suppressed. Figure 1b shows the spectrum fragment in the low-amplitude region, measured with higher amplification. In this region the lines of X-rays with different energies corresponding to the absorption in the bottom electrode are also visible.

Figure 2 shows the dependences of the signal amplitude on the absorbed X-ray energy. The signals of the top and bottom electrodes are denoted by Q_{top} and Q_{base}, respectively. The data for the top electrode (squares in the line 1) exhibit the nonlinearity of response and are characterized by negative curvature. Such behavior is caused by self-recombination of excess quasiparticles in the top electrode [4]. Squares in the line 2 show the data for the bottom killed electrode. One can see that the signals of the killed electrode also nonlinearly depend on the X-ray energy; however, in this case, the dependence exhibits the positive curvature.

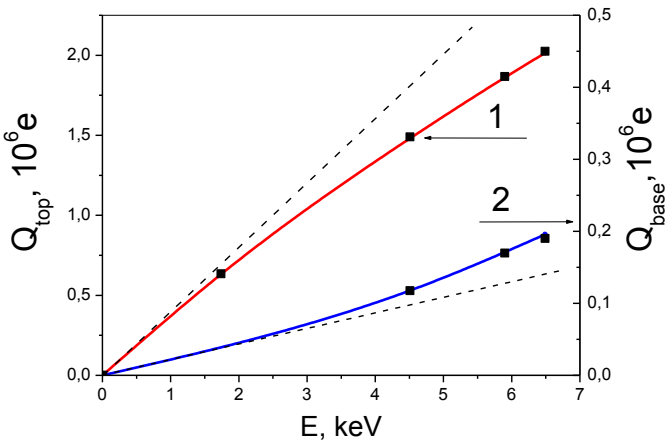

Fig. 2. Dependences of the signal amplitude on the X-ray energy for the top electrode (*1*) and the bottom electrode (*2*); V_d =0.59 mV. Squares are the experimental data. Solid lines are the diffusion model calculations. Dash lines show the linear response.

3. ANALYSIS OF THE DATA

In the analysis of experimental data, three basic mechanisms were considered: (a) multiple tunneling of quasiparticles, (b) quasiparticle tunneling from the energy trap region. (c) 2Δ-phonon exchange accompanying recombination of excess quasiparticles. All data were considered for signals of both killed and main electrodes.

Multiple tunneling of quasiparticles. To calculate the tunneling rate γ_T and the loss rate γ_L in multilayer electrodes, the proximity theory should be used [5]. Unfortunately, we are not aware of any calculations or experimental data concerning the proximity effect in Nb–Ti bi-layers. For Ti, there are also no calculations of the electron–phonon coupling constant τ_0 that defines the scale of the relaxation rate γ_{Trap} [6]. Therefore, we present only some estimates.

The tunneling probability P_{top} for the top electrode was estimated from the signal amplitude, $P_{top} \approx 0.65$. For the killed electrode the tunneling rate was estimated from the total electrode thickness $d_{base} = d_b(Nb) + d_b(Ti)$: $\gamma_{T\text{-}base} \approx 0.7\ \mu s^{-1}$. The main loss process in the killed electrode is the quasiparticle trapping in the Ti layer region. Trapping rate was estimated as $\gamma_{Trap} \approx 0.5\ ns^{-1}$. As the result, $P_{base} \approx 0.002$. Accordingly the signal amplitudes should be $Q_{base} \approx 6 \cdot 10^3$ e and $Q_{top} \approx 2.4 \cdot 10^6$ e [1]. However, the experiment yields ten times higher amplitudes for the bottom electrode, $Q_{base}(exp) \approx (14–22) \cdot 10^4$ e. The multiple tunneling mechanism can not cause the detector nonlinearity with respect to X-ray energy also. Thus multiple tunneling is insufficient to explain experimental data.

Tunneling from the trap. According to the proximity effect theory [5], the superconducting gap Δ_g in multilayer structures is identical for all layers. Hence, in the killed Ti/Nb electrode near the tunnel barrier, there exist quasiparticle states at low energies, which correspond to energies in the Ti-trap. The density of these states is exponentially small. Nevertheless, excess quasiparticles have a certain probability to tunnel from these levels, particularly in the case of thin electrodes [7]. In samples under study the Nb and Ti layers were thick as compared with coherence lengths. As a result, the contributions of this process are expected to be very small.

Phonon exchange mechanism. A significant contribution to the bottom electrode signal can be made by the phonon exchange mechanism. The quasiparticles resulting from X-ray absorption have high density, which causes their recombination and emission of 2Δ-phonons. A part of 2Δ-phonons go out to the opposite electrode and produce excess quasiparticles, whose tunneling additionally contributes to the signal. Since the phonon contribution is caused by self-recombination, it depends quadratically on the initial number of quasiparticles N_0, i.e., on the X-ray absorption energy. In

contrast to the top electrode signal, where recombination results in signal attenuation (line 1 in Fig. 3), the recombination in the bottom electrode increases the resulting signal. As a result, the energy dependence of the bottom electrode signal Q_{base} should have the positive curvature (line 2 in Fig. 3).

In figure 2 the solid lines show the calculation within a diffusion model. The movement of the excess quasiparticles in both electrodes was described by the system of differential diffusion equations which included processes of tunneling, losses and self-recombination of quasiparticles. The calculations were performed by numerical methods. One set of parameters describes the experimental data for two electrodes, including the different curvature of the curves for the top and bottom electrodes. Thus, the experimental data suggest that the self-recombination and phonon exchange make a significant contribution to the killed electrode signal.

What are recommendations on reducing the killed electrode signal? The tunneling contribution is controlled by the quasiparticle trapping rate γ_{Trap}, which depends on electrode materials and the trap depth. It is important to provide the maximum trap depth, which yields the maximum rate γ_{Trap}. These conditions are satisfied at $d_{Nb} >> \xi(Nb)$ and $d_{Ti} > \xi^*(Ti)$.

To reduce the main contribution of 2Δ-phonon exchange, self-recombination of quasiparticles should be weakened. The recombination loss ΔN_R is inversely proportional to the squared thickness d_b [8]. Therefore, the simplest method for decreasing $\Delta Q_{base\text{-}R}$ is an increase of the electrode

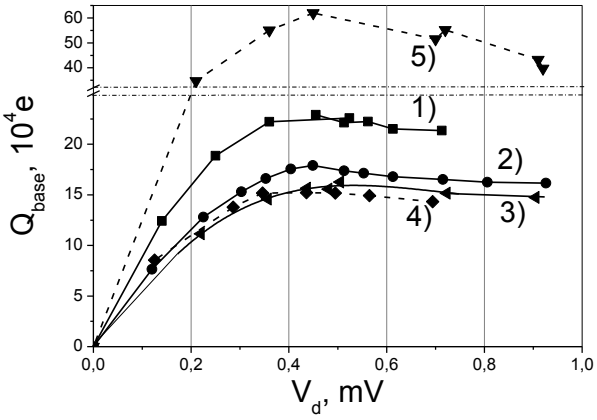

Fig. 3. Signal amplitudes of Nb–Ti (*1–4*) and Nb–Al (*5*) killed electrodes in STJ detectors as functions of the voltage V_d for samples with electrode thicknesses d_{base}, d_{top}, and $d_{Al(2)}$: (*1*) 130, 193, and 13 nm; (*2*) 180, 243, and 13 nm; (*3*) 180, 293, and 13 nm; (*4*) 180, 243, and 12; (*5*) 90, 145, and 15 nm.

thickness d_b. Figure 3 shows the killed electrode signals as a function of the voltage V_d for samples differing by thicknesses of top and bottom electrodes. Lines 1–4 are the data on (Nb/Ti) detectors; line 5 presents the data for similar detectors with killed Nb/Al electrodes [7]. One can see that thickening of the bottom electrode results in the decrease of its signal. At the same time, the top electrode thickness has no appreciable effect on the signal Q_{base}.

5. CONCLUSION

The residual signals of the killed electrode in STJ-detectors Ti/Nb/Al,AlO_x/Al/Nb/NbN have the amplitudes at the level up to 10% of the main signal, and complicates the low-energy X-ray detection. The analysis of the experimental data shows that the 2Δ-phonon exchange between electrodes, caused by self-recombination of excess quasiparticles, yields the main contribution to the signal. Thickening of the killed electrode is an efficient method of suppression these signals.

This work was supported by the Ministry of Education and Science of the Russian Federation (contract no. 02.740.11.0242).

REFERENCES

1. P. Lerch, A. Zender, Quantum Giaever Detectors in Cryogenic Particle Detectors. Topics in Applied Physics. Christian Enss, (Editor) Springer. **99**, p. 217-265 (2005).
2. O.J. Luiten, M.L. Van den Berg, J. Gomez Rivas, M.P. Bruijn, F.B. Kiewiet, P.A.J. de Korte, Proc. of 7-th Intern. Workshop on Low Temperature Detectors, edited by S. Cooper, Munich, 1997, p. 25.
3. M.G. Kozin, I.L. Romashkina, S.A. Sergeev, L.V. Nefedov, V.A. Andrianov, V.N. Naumkin, V.P. Koshelets, L.V. Filippenko, Nucl. Instr. and Meth. in Phys. Res. A. **520**, 250 (2004).
4. V. A. Andrianov, V. P. Gorkov, V. P. Koshelets and L. V. Filippenko, Semiconductors, **41**, 215 (2007).
5. A. A. Golubov, E. P. Houwman, J. G. Gijsbertsen, J. Flokstra, H. Rogalla, J.B. le Grand and P.A.J. de Korte, Phys. Rev. B. **49**, 12953 (1994).
6. S.B. Kaplan, C.C. Chi, D.N. Landberg, J.J. Chang, S. Jafarey, D.J. Scalapino, Phys. Rev. B **14**, 4854 (1976).
7. V. A. Andrianov, M. G. Kozin, P. N. Dmitriev, V. P. Koshelets, I. L. Romashkina, and S. A. Sergeev, AIP. Conf. Proc. **605**, 161 (2002).
8. V. A. Andrianov, L. V. Filippenko, V. P. Gorkov, and V. P. Koshelets, J. Low Temp. Phys. **151**, 1049 (2008).